ANALYSIS OF NONSTEADY THERMAL MODEL OF A THIN-MEMBRANE SENSOR OF HEAT-FLUX DENSITY

A. M. Vorob'ev, V. I. Zhuk,
V. P. Sizov, and D. N. Chubarov

UDC 536.084.2

An operator comparing the nonsteady output signal of a sensor to the characteristics of the external thermal perturbation is constructed.

Circular thin-membrane sensors of heat flux density (of the type of the Gardon sensor [1]) are used to investigate the intensity of heat transfer in various elements of equipment in both full-scale and model experiments.

Structurally, the sensor is a thin constantan foil welded around the periphery of the cross section of a hollow cylinder (Fig. 1). Taken together, the elements of the sensor form two copper-constantan thermocouples: one at the center and one at the edge of the membrane. The difference in emf of the two thermocouples, which is the output signal of the sensor, may evidently be compared with some intensity characteristic of the external thermal perturbation using some operator. In the situation when the heat flux supplied is uniformly distributed over the membrane radius, the difference in emf is directly proportional to the heat flux density in steady conditions. With standard calibration of the given sensors by means of radiational heating, the sensor itself emits a relatively small radiant flux, and therefore the temperature gradient along the membrane does not play a significant role in the radiant heat transfer. The use of sensors of the given type with calibration characteristics obtained on heating by radiant fluxes in conditions of convective heat transfer may lead to marked errors because of the significant temperature gradients along the membrane, as shown in [1-4].

In [2, 4], recommendations were given, on the basis of investigations, allowing the nonlinearity of the calibration characteristics in conditions of mixed heat transfer to be taken into account. The picture is evidently significantly complicated when using such sensors in nonsteady conditions. For a correct interpretation of the measurement data in this case, analysis of the properties of the thermal model of the sensor is necessary, taking account of the set of factors influencing the formation of a nonsteady temperature field in structural elements of the sensor. In fact, without such investigations, it is difficult to judge exactly what actual characteristics of heat-transfer intensity are measured by these sensors. From a priori considerations, it may simply be assumed that the measurable emf difference evidently corresponds to some integral (over the time and the membrane surface) characteristics of the thermal perturbation.

For analysis of the sensor behavior in nonsteady conditions, consider a thermal model of the sensor (Fig. 1), including a thin membrane in ideal thermal contact over its periphery with the end of a hollow copper cylinder, the lateral surface of which is assumed to be heat-insulated. In addition, the height of the copper cylinder is assumed to be sufficiently large so that it may be regarded as thermally "thick"; it is assumed that the radius ratio R_1/R_2 allows the temperature field in the cylinder to be regarded as one-dimensional; the temperature difference over the membrane thickness and the influence of the copper wire welded to the center of the membrane on the temperature field of the membrane are neglected. The heat flux supplied to the membrane is assumed to be symmetric relative to the sensor axis and to vary arbitrarily over the radius; the heat-flux distribution in the contact zone of the membrane with the cylinder is assumed to be uniform.

The mathematical model in this case is described by the following system of heat-conduction equations, boundary and initial conditions:

Translated from Inzhenerno-Fizicheskii Zhurnal, Vol. 58, No. 2, pp. 264-270, February, 1990. Original article submitted September 2, 1988.

0022-0841/90/5802-0203$12.50

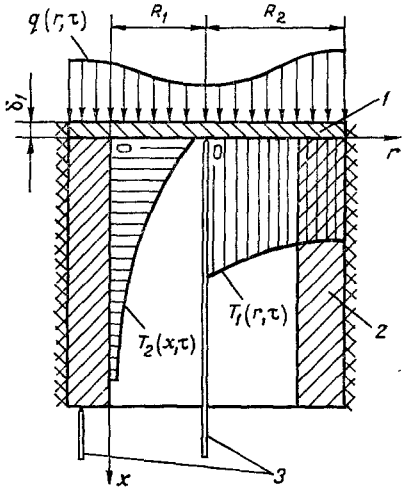

Fig. 1. Sensor construction: 1) constantan membrane; 2) copper cylinder; 3) copper electrodes.

$$\frac{\partial^2 T_1(\bar{r},\ \mathrm{Fo})}{\partial \bar{r}^2}+\frac{1}{\bar{r}}\frac{\partial T(\bar{r},\ \mathrm{Fo})}{\partial \bar{r}}+\frac{q(\bar{r},\ \mathrm{Fo})R_1^2}{\lambda_1\delta_1}=\frac{\partial T(\bar{r},\ \mathrm{Fo})}{\partial\,\mathrm{Fo}},\quad 0\leqslant\bar{r}\leqslant 1, \tag{1}$$

$$\frac{\partial^2 T_2(\bar{x},\ \mathrm{Fo})}{\partial \bar{x}^2}=k_a\frac{\partial T_2(\bar{x},\ \mathrm{Fo})}{\partial\,\mathrm{Fo}},\quad 0\leqslant\bar{x}<\infty, \tag{2}$$

$$T_2(0,\ \mathrm{Fo})=T_1(1,\ \mathrm{Fo}), \tag{3}$$

$$-\lambda_2\frac{\partial T_2(\bar{x},\ \mathrm{Fo})}{\partial \bar{x}}\bigg|_{\bar{x}=0}=R_1q_2(\mathrm{Fo})-\lambda_1\gamma_0\frac{\partial T_1(\bar{r},\ \mathrm{Fo})}{\partial \bar{r}}\bigg|_{\bar{r}=1}-\lambda_1\frac{\delta_1}{R_1}\frac{dT_1(1,\ \mathrm{Fo})}{d\,\mathrm{Fo}}, \tag{4}$$

$$T_2(\bar{x},\ \mathrm{Fo})_{\bar{x}\to\infty}=0;\ T_1(\bar{r},\ 0)=T_2(\bar{x},\ 0)=0. \tag{5}$$

Using Laplace transformation with respect to Fo, the following relations may be written in the mapping space

$$\frac{d^2T_1(\bar{r},\ s)}{d\bar{r}^2}+\frac{1}{\bar{r}}\frac{dT_1(\bar{r},\ s)}{d\bar{r}}-sT_1(\bar{r},\ s)+\frac{q(\bar{r},\ s)R_1^2}{\lambda_1\delta_1}=0, \tag{6}$$

$$\frac{d^2T_2(\bar{x},\ s)}{d\bar{x}^2}=k_asT_2(\bar{x},\ s), \tag{6'}$$

$$-\lambda_2\frac{dT_2(\bar{x},\ s)}{\partial \bar{x}}\bigg|_{\bar{x}=0}=R_1q(s)-\lambda_1\gamma_0\frac{dT_1(\bar{r},\ s)}{\partial \bar{r}}\bigg|_{\bar{r}=1}-\lambda_1\frac{\delta_1}{R_1}sT_1(1,\ s), \tag{7}$$

$$T_2(0,\ s)=T_1(1,\ s),\ T_2(\bar{x},\ s)_{\bar{x}\to\infty}=0. \tag{8}$$

It may be shown that the general solution of Eq. (6) takes the form

$$T_1(\bar{r},\ s)=AI_0(\sqrt{s}\bar{r})+K_0(\sqrt{s}\bar{r})\int_0^{\bar{r}}\xi\tilde{q}(\xi,\ s)I_0(\sqrt{s}\xi)\,d\xi+\ I_0(\sqrt{s}\bar{r})\int_{\bar{r}}^1\xi\tilde{q}(\xi,\ s)K_0(\sqrt{s}\xi)\,d\xi, \tag{9}$$

$$\tilde{q}(\xi,\ s)=\frac{R_1^2}{\lambda_1\delta_1}q(\xi,\ s).$$

From the solution in Eq. (9), it follows that

$$T_1(\bar{r},\ s)=[I_0(\sqrt{s})-1]^{-1}I_0(\sqrt{s}\bar{r})\left\{\int_0^1\xi\tilde{q}(\xi,\ s)K_0(\sqrt{s}\xi)\,d\xi-K_0(\sqrt{s})\int_0^1\xi\tilde{q}(\xi,\ s)I_0(\sqrt{s}\xi)\,d\xi\right\}+K_0(\sqrt{s}\bar{r})\int_0^{\bar{r}}\xi\tilde{q}(\xi,\ s)\times$$

$$\times I_0(\sqrt{s}\xi)\,d\xi+I_0(\sqrt{s}\bar{r})\int_{\bar{r}}^1\xi\tilde{q}(\xi,\ s)K_0(\sqrt{s}\xi)\,d\xi-\frac{\Delta T(s)I_0(\sqrt{s}\bar{r})}{I_0(\sqrt{s})-1}, \tag{10}$$

where $\Delta T(s) = T_1(0, s) - T_1(1, s)$.

If $\tilde{q}(\bar{r}, s)$ is written in the form

$$\tilde{q}(\bar{r}, s) = \tilde{q}_0(s) + \Delta\tilde{q}(\bar{r}, s), \tag{11}$$

the following result is obtained on taking account of the well-known relations [5] for integrals of Bessel functions, after a series of identical transformations

$$T_1(\bar{r}, s) = \tilde{q}_0(s)/s + K_0(\sqrt{s}\bar{r}) \int_0^{\bar{r}} \xi\Delta\tilde{q}(\xi, s) I_0(\sqrt{s}\xi)\, d\xi +$$
$$+ I_0(\sqrt{s}\bar{r}) \int_{\bar{r}}^{1} \xi\Delta\tilde{q}(\xi, s) K_0(\sqrt{s}\xi)\, d\xi + I_0(\sqrt{s}\bar{r}) [I_0(\sqrt{s}) - 1]^{-1} \times \tag{12}$$
$$\times \left\{ \int_0^1 \xi\Delta\tilde{q}(\xi, s) K_0(\sqrt{s}\xi)\, d\xi - K_0(\sqrt{s}) \int_0^1 \xi\Delta\tilde{q}(\xi, s) I_0(\sqrt{s}\xi)\, d\xi \right\} - \Delta T(s) I_0(\sqrt{s}\bar{r}) [I_0(\sqrt{s}) - 1]^{-1}$$

and when $\bar{r} = 1$

$$T_1(1, s) = \tilde{q}_0(s)/s + [I_0(\sqrt{s}) - 1]^{-1} \int_0^1 \xi\Delta\tilde{q}(\xi, s) \times \tag{13}$$
$$\times [I_0(\sqrt{s}) K_0(\sqrt{s}\xi) - K_0(\sqrt{s}) I_0(\sqrt{s}\xi)]\, d\xi - \Delta T(s) I_0(\sqrt{s}) [I_0(\sqrt{s}) - 1]^{-1}.$$

In turn, the solution of Eq. (6') in Laplacian mapping space takes the form

$$T_2(\bar{x}) = T_1(1, s) \exp(-k_a^{1/2}\sqrt{s}\bar{x}). \tag{14}$$

Using the expression for $dT_1/d\bar{r}$ from Eq. (12) and that for $dT_2/d\bar{x}$ from Eq. (14), and substituting the relations obtained in Eq. (7), it is found that

$$\lambda_2 k_a^{1/2}\sqrt{s} T_1(1, s) = q_2(s) R_1 - \lambda_1\gamma_0 [\Psi_1(s) - \sqrt{s}\Delta T(s) I_1(\sqrt{s})] [I_0(\sqrt{s}) - 1]^{-1} - \lambda_1\delta_1/R_1 s T_1(1, s), \tag{15}$$

where

$$\Psi_1(s) = \sqrt{s} \int_0^1 \xi\Delta\tilde{q}(\xi, s) [K_1(\sqrt{s}) I_0(\sqrt{s}\xi) + I_1(\sqrt{s}) K_0(\sqrt{s}\xi)]\, d\xi - \int_0^1 \xi\Delta\tilde{q}(\xi, s) I_0(\sqrt{s}\xi)\, d\xi.$$

It follows from Eq. (15) that

$$T_1(1, s) = [\lambda_2 k_a^{1/2}\sqrt{s} + \lambda_1 s\delta_1/R_1]^{-1} \{q_2(s) R_1 - [I_0(\sqrt{s}) - 1]^{-1} [\gamma_0\lambda_1\Psi_1(s) - \gamma_0\lambda_1\sqrt{s} I_1(\sqrt{s})\Delta T(s)]\}. \tag{16}$$

Substituting Eq. (16) into Eq. (13), and taking account of the expression for $\Psi_1(s)$ and the relations $\tilde{q}_0(s) = q_0(s)R_1^2/(\lambda_1\delta_1)$; $\Delta\tilde{q}(s) = \Delta q(s)R_1^2/(\lambda_1\delta_1)$ when $q_0(s) = q_2(s)$, it is found that

$$\frac{q_0(s)}{s} + [I_0(\sqrt{s}) - 1]^{-1} \left\{ \gamma_0\varepsilon \left(\int_0^1 \xi\Delta q(\xi, s) [K_1(\sqrt{s}) I_0(\sqrt{s}\xi) + I_1(\sqrt{s}) K_0(\sqrt{s}\xi)]\, d\xi - \right.\right.$$
$$\left. - \frac{1}{\sqrt{s}} \int_0^1 \xi\Delta q(\xi, s) I_0(\sqrt{s}\xi)\, d\xi \right) + \left(1 + \sqrt{s}\varepsilon \frac{\delta_1}{R_1}\right) \int_0^1 \xi\Delta q(\xi, s) [I_0(\sqrt{s}) K_0(\sqrt{s}\xi) - K_0(\sqrt{s}) I_0(\sqrt{s}\xi)]\, d\xi \left.\right\} = \tag{17}$$

$$= \frac{\lambda_1\delta_1}{R_1^2}\Delta T(s) \left[I_0(\sqrt{s}) + \varepsilon \frac{\delta_1}{R_1}\sqrt{s} I_0(\sqrt{s}) + \gamma_0\varepsilon I_1(\sqrt{s}) \right] \Big/ [I_0(\sqrt{s}) - 1].$$

Equation (17) may be written in the form

$$B(s)\Delta T(s) = \frac{q_0(s)}{s} + A_1(s)\Delta q(s) + A_2(s)\Delta q(s), \tag{18}$$

where A_1, A_2, and B are operators expressed by the corresponding terms of the functional relation in Eq. (17). In the untransformed space, evidently, A_1, A_2 are some integral operators with respect to time and space; B is an integral operator with respect to the time. It is clear from Eqs. (17) and (18) that the measurable temperature difference ΔT may, in the general case, be compared with some integral characteristics of the external thermal perturbation, including both actual values of the heat fluxes supplied and terms taking account of the previous history of the process and the nonuniformity of heat transfer over the men-

brane radius. In the situation where it is known from a priori considerations that $\Delta q = 0$, the experimental temperature difference ΔT may be compared, using the operator B, with the actual heat-flux values, taking account of nonsteady effects due to the set of factors of the process by which nonsteady temperature fields are formed in a sensor of the given type. Neglecting these factors may lead to incorrect interpretation of the measurement data. It is evident that the level of error which arises on account of neglecting nonsteady effects may be judged on the basis of a comparison of the functional relation obtained for ΔT and that realized in steady conditions with constant temperature at the periphery of the membrane.

Equation (13) is now written in the form

$$T_1(1, s)[I_0(\sqrt{s}) - 1] = \frac{\tilde{q}_0(s)}{s}[I_0(\sqrt{s}) - 1] + \\ + \int_0^1 \xi \Delta\tilde{q}(\xi, s)[I_0(\sqrt{s}) K_0(\sqrt{s}\xi) - K_0(\sqrt{s}) I_0(\sqrt{s}\xi)]\, d\xi - \Delta T(s) I_0(\sqrt{s}). \tag{19}$$

In the case where $\tilde{q}_0(s)$, $\Delta\tilde{q}(\xi, s)$ do not depend on the time and the temperature is maintained constant at the periphery of the membrane, it is found on the basis of the limiting relation $\lim_{s\to 0} F(s)s = F(\tau)_{\tau\to\infty}$, taking account of the asymptotic estimates of $I_0(\sqrt{s})$, $K_0(\sqrt{s})$ as $s \to 0$, that

$$q_0 - 4\int_0^1 \xi \Delta q(\xi) \ln \xi d\xi = 4\frac{\lambda_1\delta_1}{R_1^2}\Delta T. \tag{20}$$

Thus, Eq. (20) is a functional relation between the temperature difference and the incoming heat flux with an arbitrary distribution of the flux over the membrane radius, in steady conditions realized with $T_1(1, \tau) = \text{const}$.

When using the calibration characteristics of sensors of the given type obtained with the heat flux uniformly distributed over the membrane surface to interpret measurement data, it must be remembered that the sensor output signal in steady conditions corresponds to some integral (over the surface, with weight $\xi \ln \xi$) values of the actual incoming heat fluxes. With information regarding the specific heat-flux distribution over the membrane surface, it may be concluded, in principle, precisely which point of the membrane corresponds to the sensor output signal, if some constant temperature is maintained at its periphery. Thus, assuming a quadratic law of the heat-flux distribution over the radius

$$q(\bar{r}) = q_0 - \Delta q^*(1 - \bar{r}^2),$$

it follows that in steady conditions

$$q_0 - \frac{3}{4}\Delta q^* = 4\frac{\lambda_1\delta_1}{R_1^2}\Delta T \tag{21}$$

and hence the sensor output signal corresponds to the heat flux at the point of the membrane with radius $\bar{r} = 1/2$.

Conclusions regarding the interpretation of the measurement data using standard calibration characteristics may be reached on the basis of a comparison of the functional relation in Eq. (20) and Eq. (17), after inverse transformation.

In the untransformed space, Eq. (17) may be written in the form

$$q_0(\mathrm{Fo}) + Q_1^*(\mathrm{Fo}) + Q_2^*(\mathrm{Fo}) = \frac{\lambda_1\delta_1}{R_1^2}\frac{d}{d\mathrm{Fo}}\varphi(\mathrm{Fo}), \tag{22}$$

where Q_1^* and Q_2^* correspond to the mappings in the curly brackets on the left-hand side of Eq. (17), multiplied by s. The function $\phi(\mathrm{Fo})$ corresponds to the transform

$$\varphi(s) = \varphi_1(s) + \varphi_2(s) + \varphi_3(s), \tag{23}$$

where $\varphi_1(s) = I_0(\sqrt{s})[I_0(\sqrt{s}) - 1]^{-1}\Delta T(s)$; $\varphi_2(s) = \varepsilon\delta_1/R_1\sqrt{s}\, I_0(\sqrt{s})[I_0(\sqrt{s}) - 1]^{-1}\Delta T(s)$; $\varphi_3(s) = \varepsilon\gamma_0 I_1(\sqrt{s})[I_0(\sqrt{s}) - 1]^{-1}\Delta T(s)$.

The functions ϕ_1, ϕ_2, ϕ_3 for times $n\Delta\mathrm{Fo}$ ($n \geq 1$) may be approximated in the form

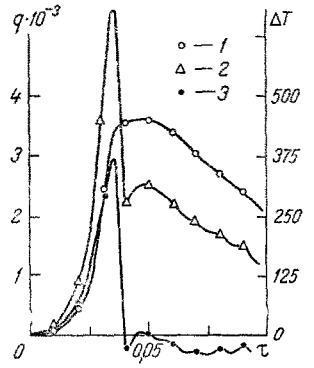

Fig. 2. Results of numerical experiment: 1) model temperature (output signal of sensor), K; 2) actual heat-flux density, $kW \cdot m^{-2}$; 3) error in determining the heat flux using a standard calibration, $kW \cdot m^{-2}$.

$$\varphi_1(n\Delta Fo) = \Delta T(n\Delta Fo) + \frac{1}{2}\sum_{j=1}^{n}\{\Delta T[(n-j+1)\Delta Fo] + \Delta T[(n-j)\Delta Fo]\}\{C_1[j\Delta Fo] - C_1[(j-1)\Delta Fc]\};$$

$$\varphi_2(n\Delta Fo) = \varepsilon\delta_1/R_1\sum_{j=1}^{n}\Delta T'[(n-j+1)\Delta Fo]\{C_2[j\Delta Fo] - C_2[(j-1)\Delta Fo]\};$$

$$\varphi_3(n\Delta Fo) = \varepsilon\gamma_0\sum_{j=1}^{n}\Delta T'[(n-j+1)\Delta Fo]\{C_3[j\Delta Fo] - C_3[(j-1)\Delta Fo]\},$$

where C_1, C_2, C_3 correspond to the transforms

$$C_1(s) = s^{-1}\sum_{k=1}^{\infty} I_0^{-k}(\sqrt{s});\ C_2(s) = s^{-1/2}I_0(\sqrt{s})C_1(s);$$

$$C_3(s) = s^{-1}I_1(\sqrt{s})C_1(s),$$

inverse transformation of which is by the well-known inversion theorem [6], including the systematic application of the theorem on the convolution of the untransformed functions.

On the basis of Eq. (22) and (20)

$$\Delta\tilde{Q}(Fo) = \frac{\lambda_1\delta_1}{R_1^2}\frac{d}{dFo}\varphi(Fo) - 4\frac{\lambda_1\delta_1}{R_1^2}\Delta T(Fo), \qquad (24)$$

where $\Delta\tilde{Q}(Fo)$ evidently characterizes the error arising on account of neglecting nonsteady effects.

On the basis of the expression obtained for the operator comparing the experimental $\Delta T(\tau)$ with the characteristics of the external thermal perturbation, computational algorithms realized on a computer may be developed. Using programs developed for a computer, a numerical simulational experiment is undertaken to estimate the error arising on account of neglecting nonsteady effects when using standard calibration curves. The results of one such experiment are shown in Fig. 2. The geometric characteristics of the sensor here are assumed to be as follows: $R_1 = 0.7$ mm, $R_2 = 3.5$ mm, $\delta_1 = 0.03$ mm. The membrane material is constantan with $\lambda_1 = 0.0232\ kW \cdot m^{-1} \cdot K^{-1}$; $a_1 = 0.636 \cdot 10^{-5}\ m^2 \cdot sec^{-1}$; $c_1\rho_1 = 3649\ kJ \cdot m^{-3} \cdot K^{-1}$; the cylinder material is copper with $\lambda_2 = 0.37\ kW \cdot m^{-1} \cdot K^{-1}$; $a_2 = 1.06 \cdot 10^{-4}\ m^2 \cdot sec^{-1}$; $c_2\rho_2 = 3489\ kJ \cdot m^{-3} \cdot K^{-1}$. The nonsteady output signals of the sensor $\Delta T(\tau)$ in Fig. 2 are assumed to correspond to the case of a uniform distribution of $q(\bar{r}, \tau)$ over the membrane surface, i.e., $\Delta q(\bar{r}, \tau) = 0$. In these conditions, the value of $\Delta\tilde{Q}(\tau)$ corresponding to Eq. (24) evidently characterizes the difference between the actual values of $q(\tau)$ and those obtained using the standard calibration curve. As follows from Fig. 2, for significantly nonsteady sensor output signals $\Delta T(\tau)$, the error level determined by Eq. (24) may be sufficiently significant, indicating the need to take account of nonsteady effects in interpreting measurements data for sensors of the given type in conditions of short-term, significantly nonsteady, and highly intense heat-transfer processes.

NOTATION

r, x, coordinates; $\bar{r} = r/R_1$, $\bar{x} = x/R_1$, dimensionless coordinates; τ, time; $Fo = a_1\tau/R_1^2$, Fourier number; λ_1, a_1, c_1, ρ_1, λ_2, a_2, c_2, ρ_2, thermal conductivity, thermal diffusivity, specific heat, density of membrane material and cylinder, respectively; δ_1, membrane thickness; $k_a = a_1/a_2$; $\varepsilon = [\lambda_1 c_1 \rho_1/(\lambda_2 c_2 \rho_2)]^{1/2}$; $\gamma_0 = 2\delta_1 R_1 R_2^{-2}\,[1 - (R_1/R_2)]^{-1}$; $q(r, \tau)$, heat flux; $T_1(r, \tau)$, $T_2(x, \tau)$, temperature of membrane and cylinder; $I_0(z)$, $I_1(z)$, $K_0(z)$, $K_1(z)$, modified Bessel functions and MacDonald functions (of zero and first order).

LITERATURE CITED

1. R. Gardon, ASME, J. Heat Trans., 82, 396-398 (1960).
2. Strigl and Diller, Teplopered, No. 1, 25-33 (1984).
3. Vudroff, Khiern, and Kelikher, Raket. Tekh. Kosmonavt., No. 4, 240-242 (1967).
4. Borell and Diller, Teplopered., No. 1, 82-90 (1987).
5. Bateman and Erdeii, Higher Transcendental Functions [Russian translation], Moscow (1966).
6. A. V. Lykov, Theory of Heat Conduction [in Russian], Moscow (1967).

CONTROL OF CEMENTATION THROUGH A CONTINUOUS CHANGE IN CARBON POTENTIAL AND TEMPERATURE IN A GAS FURNACE

V. D. Kal'ner, S. A. Yurasov,
V. B. Glasko, N. I. Kulik,
Yu. K. Evseev, and A. N. Tikhonov

UDC 539.219.3

A numerical experiment is conducted to study the feasibility of automatic control of cementation through a continuous change in carbon potential and the temperature of the external medium.

1. The idea of controlling the saturation process during cementation by changing the parameters of the furnace atmosphere over time was first proposed in [1]. The authors of [1, 2] examined simple control methods in which the carbon potential of the external medium decreases suddenly at a certain moment. They addressed the question of choosing this moment so that the resulting distribution of carbon in the diffusion layer is as close as possible to a profile with a plateau corresponding to a constant concentration.

The problem of controlling the process with a continuous change in carbon potential over time was solved in [3, 4] by the method of mathematical modeling. It was shown through a mathematical experiment in [3] that changing the duration of the transitional stage makes it possible to regulate the effective thickness of the layer and to approximately attain the necessary carbon distribution in less time. The mathematical notion of regularization [5] was used in [4] to solve the control problem by varying carbon potential. This approach made it possible to fully automate calculation of the optimum control function on a computer.

Here, we make the first attempt to mathematically model the production process (PP) when it is controlled simultaneously by a time change in the carbon potential and the temperature of the saturating atmosphere of the furnace. The control functions were chosen from a class of functions that permits simple realization (Fig. 1) and were parameterized accordingly.

Nomograms were developed in [6] for the simplest method of control – by changing the carbon potential over time. The nomographic method of describing functional relations is especially effective when the functions are explicitly given [7]. However, with the large number of control parameters in our case and the implicit character of the relationship be-

Moscow State University. Translated from Inzhenerno-Fizicheskii Zhurnal, Vol. 58, No. 2, pp. 271-278, February, 1990. Original article submitted July 6, 1988.

0022-0841/90/5802-0208$12.50